THE ASTROPHYSICAL JOURNAL, 451:298–307, 1995 September 20

SODIUM ENRICHMENT IN A–F TYPE SUPERGIANTS

MOUNIB F. EL EID
Department of Physics, American University of Beirut, Beirut, Lebanon; and Universitäts-Sternwarte, Geismarlandstr. 11, D-37083 Göttingen, Germany

AND

ARTHUR E. CHAMPAGNE
University of the North Carolina at Chapel Hill, NC 27599; and Triangle Universities Nuclear Laboratory, Duke University, Durham, NC

Received 1994 November 14; accepted 1995 March 30

ABSTRACT

We have investigated the nucleosynthesis of sodium (^{23}Na) in stars of masses $M = 5$–$19\ M_\odot$ having solar-like initial chemical composition. The values obtained for the Na excess after the first dredge-up phase are in close agreement with recent observations suggesting a moderate Na excess in F-type supergiants. We also found a positive correlation between the overabundance factors [N/H] and [Na/H] which seems to indicate that Na enrichment originates from the Ne-Na cycle operating simultaneously with the CNO tri-cycle in these stars. We emphasize that our results were obtained on the basis of standard physical assumptions in the stellar model calculations, but with updated reaction rates for the reactions involved in the Ne-Na cycle which are presented in this work.

Subject headings: nuclear reactions, nucleosynthesis, abundances — stars: evolution — stars: interiors

1. INTRODUCTION

It is still a matter of debate whether the observed Na excess in A–F type supergiants arises from products of the Ne-Na cycle that have been mixed to the surface after the first dredge-up phase. A recent determination of the Na excess in A–F supergiants, based on the equivalent widths of Na I lines, has been provided by Takeda & Takada-Hidai (1994, hereafter TT94). Their non-LTE analysis of the Na I lines indicates that the F supergiants exhibit a moderate Na excess of [Na/H] $\approx$ 0.00–0.50 ([X] = log $X_{\rm star}$ − log $X_\odot$). The observed values for [Na/H] seem to increase with stellar mass and show a positive correlation with [N/H]. For the A-type supergiants, TT94 found rather high values of [Na/H] $\approx$ 0.70–0.80 that were not correlated with the stellar mass, in contrast to the F-type supergiants. More details concerning these observations are given in § 2.

According to TT94, previous data for the Na excess derived by Boyarshuck et al. (1988) were overestimated for many F-type supergiants because of an improper treatment of the non-LTE effects. Therefore, previous attempts to explain these observations have invoked ad hoc assumptions such as increasing the initial abundances of ^{22}Ne (Denissenkov 1990), or artificially increasing the rate of the ^{20}Ne(p, γ) reaction (Prantzos, Coc, & Thibaud 1991; El Eid & Prantzos 1993).

In § 4, we will present the surface abundances for the CNO isotopes and Na predicted on the basis of evolutionary calculations for stars with initial masses $M = 5$–$20\ M_\odot$. It will be shown that the values of [Na/H] obtained by TT94 for the F-type supergiants can generally be explained on the basis of standard physical assumptions in the stellar models. We will also give estimates for the masses of the A and F supergiants listed in Table 1 on the basis of our evolutionary tracks.

In attempting to explain the Na excess in these stars, we will adopt the point of view (see also Luck & Lambert 1985) that they are post–red supergiants performing blue loops in the H-R diagram. In a previous paper (El Eid 1994b), we found that the red-blue loops did not occur for stellar masses of $M > 13\ M_\odot$, when the Schwarzschild criterion for convection was adopted. However, we have obtained these loops up to $M = 19\ M_\odot$ by adopting the Ledoux criterion for convection and combining it with semiconvective mixing. Therefore, it would be rather interesting to find out whether the observed surface abundances in these massive supergiants can help us to distinguish between these criteria for convection, and particularly to show how mixing should be treated in stellar layers having a gradient in the mean molecular weight.

In § 2, a brief summary of the recent observed data for A–F supergiants is given. The physical assumptions used in our model calculations are briefly described in § 3. In § 4, our nucleosynthesis results are presented and compared with the observed data in § 5. Concluding remarks are given in § 6.

2. OBSERVATIONS

The A–F type supergiants analyzed by TT94 are given in Table 1 together with their adopted values for log g and $T_{\rm eff}$. According to TT94, the uncertainties in $T_{\rm eff}$ or log g are assumed to be $\Delta T_{\rm eff} = T_{\rm eff}/20$ or $\Delta \log g = \pm 0.30$. The Na excess [Na/H] has been derived on the basis of the non-LTE analysis of the Na I lines including the strong line Na I λ8195. The values listed for the N excess were obtained on the basis of the N I lines and were considered by TT94 as tentative results because of the blending effect of other lines. The masses of the stars shown in Table 1 were estimated from their adopted log g and $T_{\rm eff}$ values and by using a mass-luminosity relation $L \propto M^4$. These estimates will be tested on the basis of our evolutionary tracks (see § 4).

The main features of the data shown in Table 1 are as follows.

1. The effective temperatures of the F-type supergiants lie in the range $T_{\rm eff} \approx 6000$–7500 K. These stars show moderate values of [N/H] $\approx$ 0.07–0.53 that tend to increase with the stellar mass (see also Fig. 3). Although the results for [N/H]

TABLE 1

SODIUM AND NITROGEN OVERPRODUCTION FACTORS AND STELLAR PARAMETERS

Object (1)	Spectral Type (2)	$T_{\rm eff}$ (K) (3)	log g (cm s^{-2}) (4)	[Na/H] (5)	[N/H] (6)	M^a ($M_\odot$) (7)	M^b ($M_\odot$) (8)
α UMi	F8 Ib	6000	1.50	+0.07	+0.14	10.0	9.3
η Aql.....	Cepheid	6000	1.50	+0.15	+0.04	10.0	9.3
ζ Gem	Cepheid	5750	1.50	−0.07	...	9.54	8.9
γ Cyg	F8 Ib	6100	0.55	+0.30	+0.11	21.4	20.0
α Car	F0 Ib	7500	1.50	+0.31	...	13.5	12.6
α Lep	F0 Ib	7000	1.30	+0.35	+0.70	14.5	13.5
α Per	F5 Ib	6250	0.90	+0.20	+0.38	17.0	15.9
ρ Cas	F8 Iap	6000	0.25	+0.47	...	26.3	24.5
		7200	0.45	...	...	...	26.7
δ CMa	F8 Ib	6250	0.60	+0.74	+0.33	21.4	20.0
η Leo	A0 Ib	10200	1.90	+0.35	+0.27	15.1	14.1
α Cyg	A2 Ia	10000	1.50	+0.79	+0.63	20.0	18.7
HR 2874.....	A5 Ib	8510	2.10	+0.75	+0.37	10.2	9.5
ϵ Aur	A8 Ia	7800	1.00	+0.67	+0.61	21.0	19.6

NOTE.—Values of [Na/H] and [N/H] as obtained by Takeda & Takada-Hidai (1994) for the A–F type supergiants. The stellar parameters ($T_{\rm eff}$, log g, M^a) were adopted by these authors. The masses M^b are estimated according to the present computation. For the star ρ Cas, the values for $T_{\rm eff}$ and log g given in the second entry were derived by Lobel et al. (1994).

are still uncertain, they seem to show a positive correlation with [Na/H]. On the basis of these results TT94 adopted the point of view that the Na excess in F-type supergiants may have originated from products of the Ne-Na cycle which have been mixed to the surface by envelope convection, or dredge-up. Our results presented in § 4 will indeed support this view.

2. In the case of the A type supergiants, only four stars were analyzed by TT94. Three of them show a rather large Na excess of [Na/H] $\approx$ +0.70–0.80. This excess does not appear to be correlated with mass as in the case of the F supergiants. The comparison of the [N/H] values with those of [Na/H] seems to indicate a positive correlation between these quantities.

3. STELLAR MODELS

The details of our evolutionary calculations (numerical code and physical assumptions) have been described in a previous work (El Eid 1994a). For completeness, we just mention that we have used the OPAL opacities according to Iglesias, Rogers, & Wilson (1992). We included mass loss by stellar wind on the basis of the semi-empirical formula by de Jager, Nieuwenhuijzen, & van der Hucht (1988). Some comments on the treatment of convection or semiconvection are given in § 4, and we refer to a previous paper by El Eid (1994b) for a detailed description. Since this work deals mainly with nucleosynthesis, we describe in the following the nuclear reactions that were employed in the calculations.

We used a network of thermonuclear reactions including 29 nuclei linked by 73 reactions. For hydrogen burning, we included the CNO tri-cycle, Ne-Na cycle, and Mg-Al cycle in addition to the *pp* chain. The reaction rates were primarily taken from the compilation by Caughlan & Fowler (1988, hereafter CF88). However, we used the lowest rates obtained by Landré et al. (1990) for the reactions $^{17}O(p, \alpha)$ and $^{17}O(p, \gamma)$. These rates are still ill determined (for a discussion, see El Eid 1994a).

We have used new reaction rates for the Ne-Na cycle, as described in the Appendix. These are: $^{20}Ne(p, \gamma)^{21}Na$, $^{21}Ne(p, \gamma)^{22}Na$, $^{22}Ne(p, \gamma)^{23}Na$, $^{23}Na(p, \gamma)^{24}Mg$, and $^{23}Na(p, \alpha)^{20}Ne$. The comparison of these rates with those given by CF88 is as follows.

1. No change has been suggested for the rate of $^{20}Ne(p, \gamma)$ reaction. Therefore, an artificial modification of this rate is not supported by the present experimental situation.
2. The rate of the $^{21}Ne(p, \gamma)$ reaction was found to be smaller in the temperature range relevant to our present study, i.e., $T_8 = 0.20–0.80$.
3. The rate of the $^{22}Ne(p, \gamma)$ reaction was found to be higher by a factor in excess of 1000 in the range $T_8 = 0.20–0.80$. Unfortunately, this rate is still poorly determined within this temperature range.
4. The rate of the $^{23}Na(p, \alpha)$ reaction is close to that adopted by CF88, while the $^{23}Na(p, \gamma)$ reaction rate is higher by a factor of 6–7 in the range $T_8 = 0.20–0.80$.

For helium burning, we have used the basic reactions responsible for energy production. In particular, for the $^{12}C(\alpha, \gamma)$ reaction we adopted the rate of Caughlan et al. (1985), but multiplied by a factor of 1.70 following the suggestion by Weaver & Woosley (1993).

4. EVOLUTIONARY RESULTS AND SODIUM ENRICHMENT

The initial chemical composition was assumed to be solar-like, where the chemical abundances were chosen according to Anders & Grevesse (1989). In particular, the abundances of ^{22}Ne and ^{23}Na (relative to Si = 10^6) are 2.34×10^5 and 5.74×10^4, respectively, i.e., with a ratio of 4.08 for $^{22}Ne/^{23}Na$.

In Figure 1, we have plotted the evolutionary tracks for stars with initial masses in the range $M = 5$ to 20 $M_\odot$. The evolution of these stars has been followed from the ZAMS up to the stage of shell He burning. The evolutionary details have been described in a previous paper by El Eid (1994b). In the following, some essential points relevant to the present work are summarized.

The interpretation of the supergiants included in Table 1 as post–red supergiants evolving upon blue loops in the H-R diagram obviously requires evolutionary sequences exhibiting these loops.

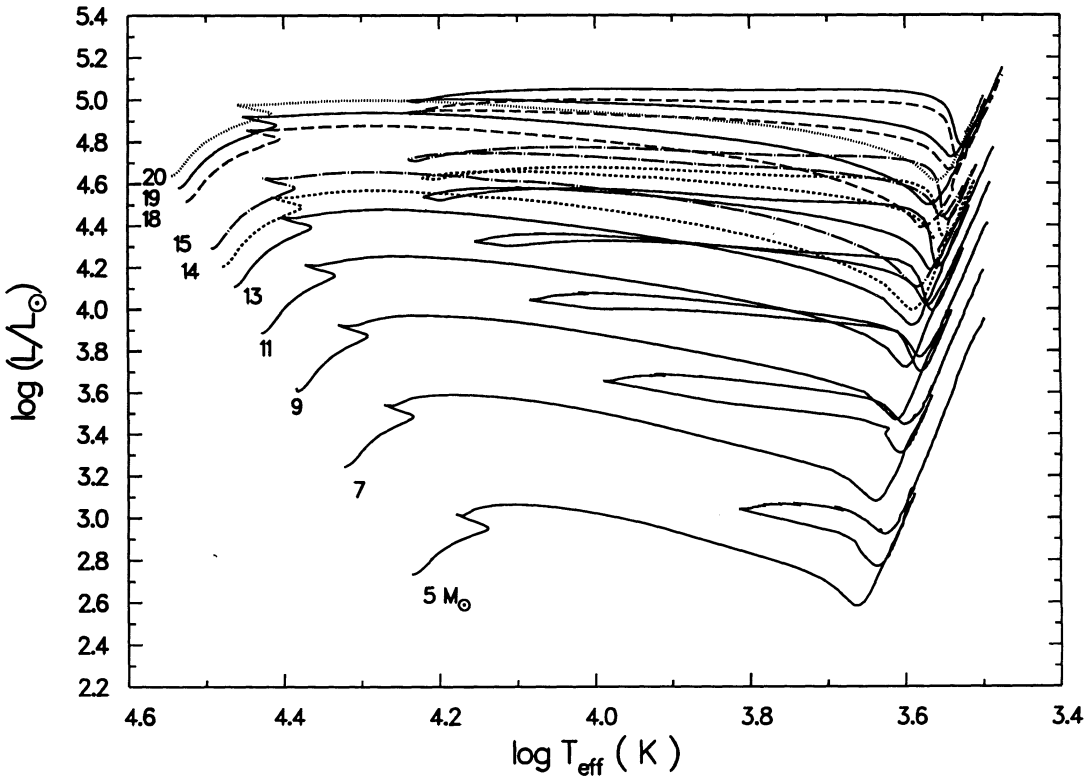

FIG. 1.—Theoretical H-R diagram showing the evolutionary tracks for initial stellar masses of M between 5 and 20 $M_\odot$. The tracks in the mass range up to $M = 13\ M_\odot$ were based on the Schwarzschild criterion for convection. Those of the higher masses were obtained with the Ledoux criterion for convection including semiconvection (see § 4).

The investigation of this issue is known to be a complicated task in stellar evolution theory (see Robertson 1972 for an early work; Stothers & Chin 1994 for a recent work). This is because many factors [such as initial composition, the treatment of convection, the rate of $^{12}C(\alpha, \gamma)^{16}O$, and mass loss] influence the properties of the blue loops.

In the recent work by El Eid (1994b), the effects of convective and semiconvective mixing on the formation and extension of the blue loops have been reinvestigated. The overall picture that has emerged from these calculations is briefly summarized as follows.

1. The properties of the blue loops depend sensitively upon the interaction between the hydrogen-burning shell and the hydrogen profile (H profile in the following) created in the model star prior to the onset of core He burning. Clearly, the shape of the H profile is rather sensitive to the treatment of convective mixing, especially in the stellar layers with a gradient in the mean molecular weight.

2. Adopting the Schwarzschild criterion for convection, i.e., by defining the convective regions according to the condition $\nabla_{rad} > \nabla_{ad}$, blue loops were easily obtained for stars of initial masses up to $M = 13\ M_\odot$ (see Fig. 1). However, no loops were found for higher masses. The basic reason for this behavior is that the Schwarzschild criterion leads to the formation of an intermediate convective zone (ICZ) prior to central helium ignition. The presence of the ICZ has two effects: first, it inhibits the inward penetration of the convective envelope to deep stellar layers; second, the hydrogen-burning shell remains relatively weak and thus no blue loop is triggered. This implies that the blue loops may be recovered if the formation of the ICZ can be avoided. This feature has also been emphasized in the work by Stothers & Chin (1994).

3. A physical way to inhibit the formation of the ICZ is to include the effect of the molecular-weight gradient (simply μ-gradient, hereafter) in the criterion for convection, that is, to eventually adopt the Ledoux criterion for convective instability. With this criterion, convective regions are defined by the condition $\nabla_{rad} > \nabla_{ad} + (\varphi/\delta)\nabla_\mu \equiv \nabla_L$, where $\nabla_\mu = d \ln \mu / d \ln P$ and the quantities φ and δ are related to the equation of state (see Kippenhahn & Weigert 1990). Clearly, the term including the μ-gradient has the net effect of inhibiting convection.

However, a complicated situation is encountered when the Ledoux criterion is adopted, namely how to treat mixing in the stellar layers in which the condition $\nabla_{ad} < \nabla_{rad} < \nabla_L$ is fulfilled. These layers are stable with respect to the Ledoux criterion, but are not with the Schwarzschild criterion. Therefore, they are dynamically stable, but vibrationally unstable. This means that the mixing in these layers may proceed on a longer timescale than does convection; they are semiconvective. There is no coherent technique in the literature for treating semiconvective mixing. In recent work (Bressan et al. 1993; Stothers & Chin 1994; Mowlavi & Foristini 1994), this type of mixing was simulated by iteratively smoothing the H profile to achieve marginal stability, i.e., to satisfy either the condition $\nabla_{rad} = \nabla_{ad}$ or $\nabla_{rad} = \nabla_L$ (Stothers & Chin 1994).

In the present work (see El Eid 1994b for more details), another approach has been used which is based on diffusive mixing. Regions that are convective according to the Ledoux

TABLE 2

PREDICTED SURFACE ABUNDANCE RATIOS (by numbers)

M	$^{12}C/^{13}C$	$^{16}O/^{17}O$	$^{16}O/^{18}O$	B $^{14}N/^{15}N$	$^{12}C/^{14}N$	[Na/Fe]	[Na/H]	[N/H]
5.....	20.29	446	634	1439	0.812	0.180	0.188	0.407
	19.70	412	643	1523	0.777	0.190	0.199	0.417
7.....	19.77	508	641	1572	0.756	0.202	0.212	0.434
	18.92	507	645	1645	0.740	0.202	0.212	0.437
9.....	19.23	576	647	1698	0.710	0.215	0.227	0.457
	18.08	540	663	1864	0.670	0.226	0.238	0.468
11.....	18.61	628	646	1893	0.644	0.237	0.256	0.497
	17.29	585	665	2113	0.603	0.249	0.268	0.509
12.....	18.14	715	644	2095	0.585	0.259	0.286	0.537
	16.50	661	665	2393	0.545	0.271	0.297	0.549
13.....	17.84	790	640	2181	0.566	0.270	0.299	0.553
	13.45	714	683	2658	0.489	0.282	0.312	0.574
15.....	17.51	805	638	2273	0.550	0.274	0.305	0.565
	16.58	606	801	3121	0.391	0.298	0.329	0.615
18.....	16.93	949	623	2460	0.519	0.293	0.332	0.597
	15.94	494	864	3789	0.323	0.383	0.423	0.663
19.....	16.73	1023	617	2539	0.506	0.300	0.343	0.611
	15.66	524	867	3970	0.310	0.400	0.443	0.679

NOTE.—Overproduction factors [Na/H], [Na/Fe], and [N/H] according to the present computation. At each initial stellar mass (in $M_\odot$), the first or second row gives the results after first dredge-up phase or second dredge-up phase.

criterion were mixed homogeneously by utilizing a large diffusion coefficient. The vibrationally unstable layers (as defined above) were mixed with a smaller diffusion coefficient, $D_{SC} = \beta D_r$, where $D_r = 4\sigma T^3/3\kappa\varrho C_P$ is the radiation diffusion coefficient (κ is the opacity and C_P is the specific heat at constant pressure), and β is an efficiency parameter. This treatment is similar to that adopted by Woosley & Weaver (1988) and Weaver & Woosley (1993). Unfortunately, it is rather difficult to obtain the parameter β from first principles. On the basis of the numerical computation by El Eid (1994b), the blue loops were obtained for stars of initial masses $13 < M/M_\odot \leq 19$ when the variation of β was confined to the interval $0.01 < \beta \leq 0.05$. The evolutionary tracks shown in Fig. 1 (for the initial masses above 13 $M_\odot$) were obtained with $\beta = 0.05$.

In comparing the present evolutionary sequences with those obtained in several recent studies (Schaller et al. 1992; Bressan

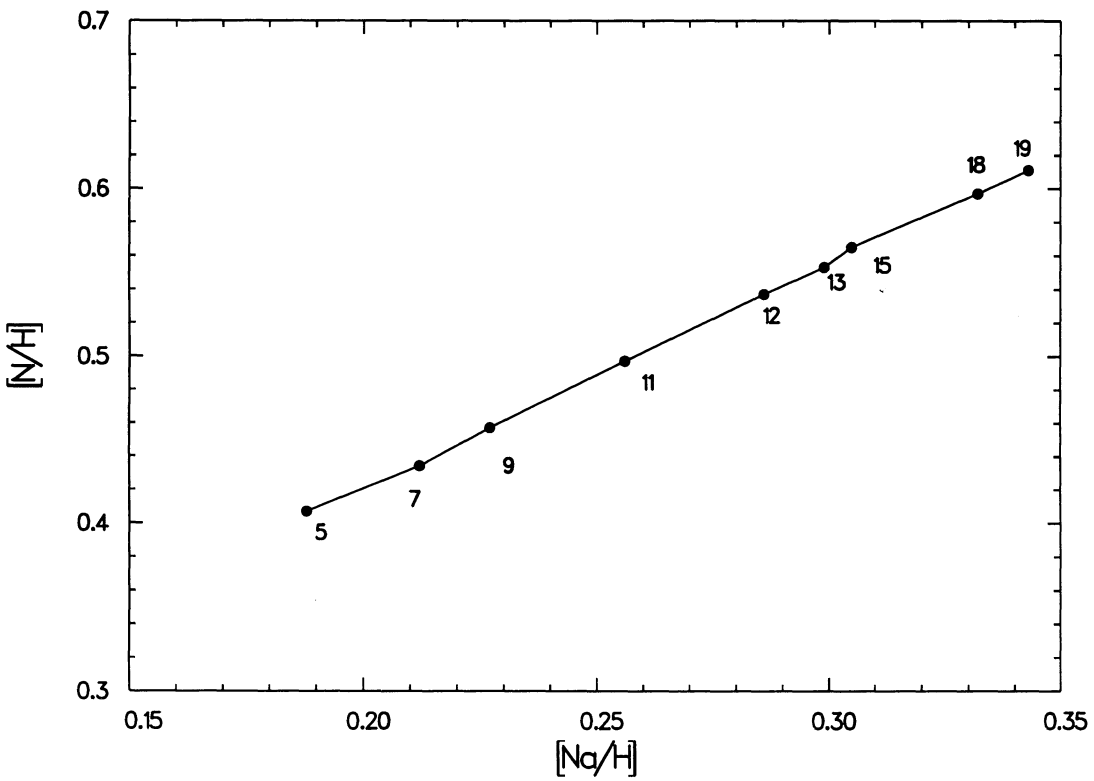

FIG. 2.—Surface nitrogen excess, [N/H], vs. sodium excess, [Na/H], predicted on the basis of the present computation. A positive correlation between N and Na is clearly seen in this diagram (see text for implications).

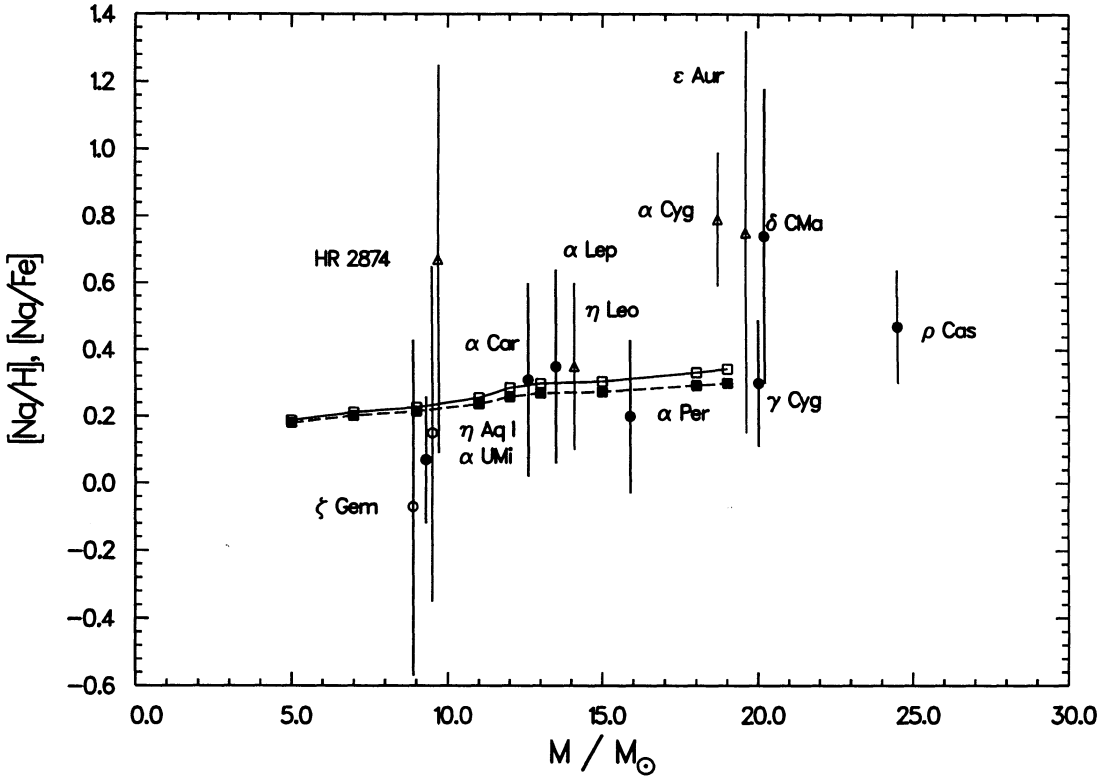

FIG. 3.—Predicted surface sodium excess, [Na/H] (*open squares*), and [Na/Fe] (*filled squares*) as a function of initial stellar mass compared with the observed values from Table 1 (for discussion see § 4). The solid and dashed lines are meant as a guide for the eyes. Note that $[X] \equiv \log X_{\rm star} - \log X_{\odot}$.

et al. 1993; Stothers & Chin 1994), we emphasize the following points.

1. In contrast to the above works, we have investigated the production of sodium by the Ne-Na cycle, especially in massive stars with initial masses above 13 $M_{\odot}$. Our aim is to understand the sodium excess observed in normal supergiants and to relate that excess to convective mixing inside such stars. We argue that understanding the correlation between the abundance anomalies observed in the atmospheres of the A–F-type supergiants and internal mixing should give more insight into the structure of massive stars during core He burning.

2. Clearly, the distribution of normal supergiants in the H-R diagram during core He burning is influenced by the presence of the blue loops. These loops in turn are highly sensitive to the treatment of mixing in the stellar layers where shell hydrogen burning occurs. Inspection of the evolutionary sequences presented by Schaller et al. (1992) and Bressan et al. (1993) reveals that the blue loops are systematically less extended or even suppressed whenever overshooting is included. In the computation by Schaller et al. (1992), where core overshooting was included, no blue loops were found for stars with initial masses $12 < M/M_{\odot} \leq 20$. In contrast, our calculations and also those by Bressan et al. (1993) and Stothers & Chin (1994) indicate that the formation of blue loops is promoted when semi-convective mixing is considered instead of overshooting.

Already this brief discussion shows that the evolution of supergiants, such as those considered in the present work, cannot be correctly described without interpretations of both the abundance anomalies observed in their atmospheres as well as how these anomalies are related to the mixing processes occurring in their interiors.

In Table 2, we summarize our predicted values for the surface abundance ratios of the CNO isotopes and the enhancement factors [Na/H], [Na/Fe], and [N/H]. These results show the expected modifications of the CNO abundances after the first and second dredge-up phases, and also clear enrichments of N and Na. In addition, the values of [Na/H] and [N/H] increase with the stellar mass, and they are correlated with each other, as can be seen in Figure 2. Note that the slope of the line drawn in this figure is $\sim 4/3$. In Figure 3, the predicted values for [Na/H] and [Na/Fe] are plotted against the stellar mass which has been estimated as described in § 5. It is seen that the difference between these quantities increases with increasing stellar mass. This reflects the effect of increasing mass loss which reduces the surface hydrogen abundance during evolution.

5. COMPARISON WITH OBSERVATIONS

5.1. *F-Type Supergiants*

Comparing the predicted values for [Na/H] (see Table 2) with those derived for the F-type supergiants collected in Table 1, we can explain the observed values for four F supergiants including the Cepheid ζ Gem. A general agreement is also obtained concerning the range of the Na excess and the positive correlation between [Na/H] and [N/H]. Still it is not clear why the Cepheid η Aql and the F star α UMi have a lower Na excess than found for ζ Gem, despite the similarity of their stellar parameters (see Table 1). The relatively high [Na/H] values proposed for the stars ρ Cas and δ CMa are clearly out

of the range of our predictions. The value for γ Cyg is within this range despite its high proposed mass. All these stars seem to be rather massive (see Table 1). If mass-loss rates that are larger than proposed by the smooth interpolation formula of de Jager et al. (1988) were used, the predicted surface abundances would eventually be modified. According to Lobel et al. (1994), hypergiants like ρ Cas seem to have mass-loss rates 3 to 30 times larger than the average rates established by de Jager et al. (1988).

It remains to be seen whether the stellar parameters ($T_{\rm eff}$, log g, M) adopted for the F supergiants in Table 1 are consistent with our evolutionary tracks shown in Figure 1. In this context, we note (C. de Jager, private communication) that the communicated g-values for very luminous stars are effective values and are rather uncertain. As an example, we have listed in Table 1 the log g, log $T_{\rm eff}$ values derived by Lobel et al. (1994) for the star ρ Cas. Therefore, by using a log g-log $T_{\rm eff}$ diagram, we calculated the log g values for a given stellar mass using the simple relation

$$\log g = -10.608 + 4 \log T_{\rm eff} + \log (M/M_\odot) - \log (L/L_\odot) . \quad (1)$$

The resulting tracks during the evolutionary phases where the blue loops occurred are plotted in Figure 4, which also show the observed supergiants listed in Table 1. It can be seen that only three F-type supergiants (ρ Cas, γ Cyg, δ CMa) are well outside the range of tracks, and all these seem to have masses in excess of 20 $M_\odot$ (see Table 1). The reason for this overall agreement is that TT94 have assumed a mass-luminosity (M-L) relation $L/L_\odot \sim (M/M_\odot)^4$ in the range log $T_{\rm eff} \sim 3.8$–4.2 K to obtain the masses listed in column (7) of Table 1. Inserting this relation into equation (1), we obtain the expression they have used, namely,

$$\log (M/M_\odot) = \tfrac{1}{3}[4 \log (T_{\rm eff}/T_{\rm eff}^\odot) - \log (g/g^\odot)] . \quad (2)$$

This expression can be improved by correcting the above M-L relation on the basis of our evolutionary tracks. In the range of log $T_{\rm eff}$ quoted above, we found the following relation:

$$(L/L_\odot) \approx 1.23(M/M_\odot)^4 , \quad (3)$$

which applies during the evolution of the stars up to their blue loops, whereupon the luminosity stays roughly constant (see Fig. 1). With this relation, the masses given in Table 1 (last column) become smaller by $\sim$0.03 dex, and this improves the agreement between predictions and observations in Figures 3 and 4.

The conclusion from this comparison is that the moderate Na excess observed in the F-type supergiants can generally be explained on the basis of standard physical assumptions in the stellar model calculations, and its origin is due to the Ne-Na cycle operating in these stars together with the CNO tri-cycle.

5.2. *A-Type Supergiants*

The interpretation of the Na excess in A-type supergiants as given in Table 1 is more complicated than in the case of the F supergiants. Only the [Na/H] value for η Leo lies in the range of our predictions, while the values for α Cyg, ϵ Aur, and HR 2874 are too high to be explained within the framework of the present standard stellar models. As argued by TT94 (in their preprint, but not in their paper), the very large overabundance of Na may be partially related to an excess of iron in these stars by 0.2–0.3 dex relative to solar. However, the discrepancy cannot be removed in this way. Other possible interpretations, such as severe mass loss on the red supergiant stage or additional mixing on the main sequence may be envisaged. At

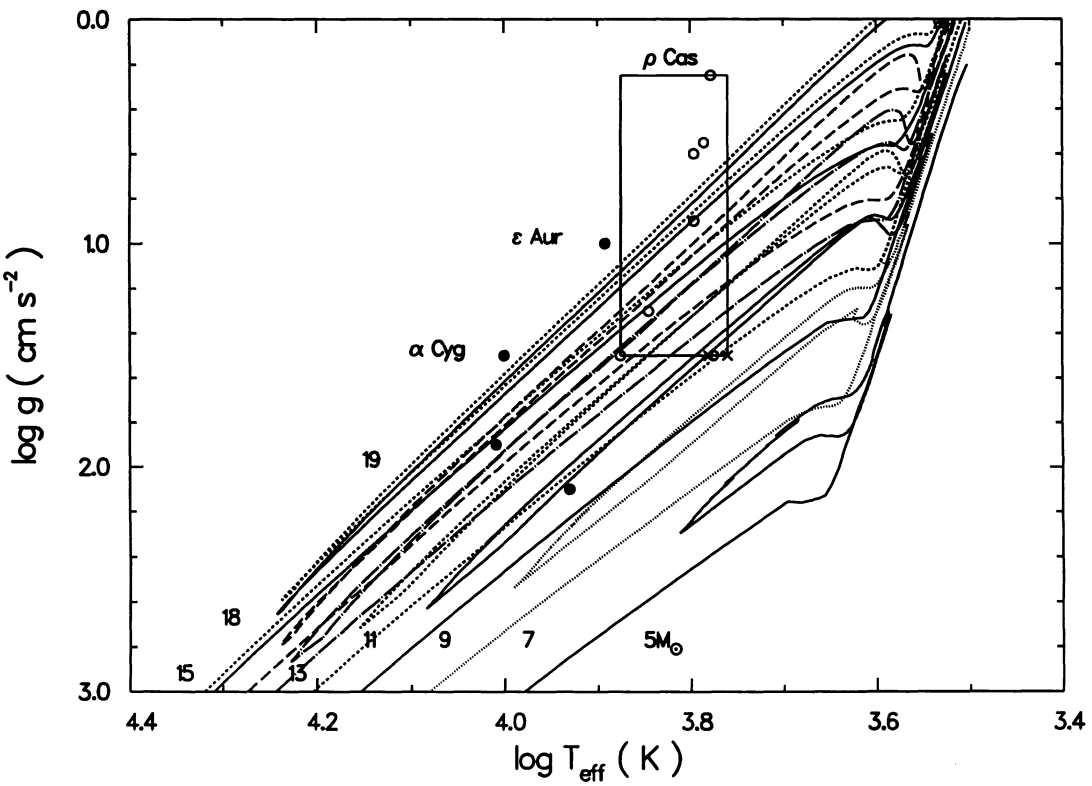

FIG. 4.—Log g vs. log $T_{\rm eff}$ diagram obtained on the basis of the evolutionary tracks displayed in Fig. 1. The inserted box indicates the range of the observed F-type supergiants according to Table 1, represented by the open circles or the crosses for the two Cepheids. The A-type supergiants are shown by the filled circles.

TABLE 3

A. Atmospheric Parameters for Three A Supergiants According to Venn (1993)

Star	Spectral Type	$T_{\rm eff}$ (K)	log g (cm s^{-2})
HD 13476.....	A3 Iab	8650 ± 200	1.70 ± 0.1
HD 87737.....	A0 Ib	9650 ± 200	1.95 ± 0.1
HD 46300.....	A0 Ib	9800 ± 200	2.15 ± 0.1

TABLE 3

B. Comparison of Predicted and Observed Overproduction Factors for A-Type Supergiants

Ratio	HD 13476	HD 87737	HD 46300	9	12A	12B	13
[C/Fe]	−0.11	−0.46	−0.34	−0.21	−0.25	−0.22	−0.23
[N/Fe]	+0.78	+0.78	+0.83	+0.44	+0.51	+0.48	+0.52
[O/Fe]	−0.20	−0.15	+0.07	−0.04	−0.06	−0.05	−0.07
[N/C]	+0.89	+1.24	+1.17	+0.66	+0.74	+0.70	+0.75
[N/O]	+0.98	+0.93	+0.76	+0.48	+0.57	+0.53	+0.59
[C + N + O/Fe].....	+0.03	+0.00	+0.14	+0.00	+0.00	+0.00	+0.00

Note.—$[X] \doteq \log X_* - \log X_\odot$. The observed values are according to Venn (1993). The predicted values are from the present computation after the first dredge-up for the 9, 12, and 13 $M_\odot$ stars (see text).

present, it seems that observational data for a larger sample of A-type stars are needed to explore these possibilities.

Other CNO abundance results have been presented by Venn (1993) for three A supergiants listed in Table 3A. Unfortunately, the Na enrichment has not been reported in this work. Nevertheless, it appears useful to compare our predictions with the data shown in Table 3B.

To obtain mass estimates for these stars, we have compared (see Fig. 5) their adopted log g and $T_{\rm eff}$ values with our evolutionary tracks for the 9, 11, and 12 $M_\odot$ stars. Figure 5 indicates that the masses lie in the range 10–12 $M_\odot$. In Table 3B, we have compared the observed CNO abundances with the predicted ones after the first dredge-up stage. For the 12 $M_\odot$ star the predicted values are given in two cases: case 12A was calculated by using the Schwarzschild criterion for convection, while case 12B was based on the Ledoux criterion including semiconvective mixing with the parameter $\beta = 0.05$ (see § 4 for details). This is to show that efficient semiconvective mixing

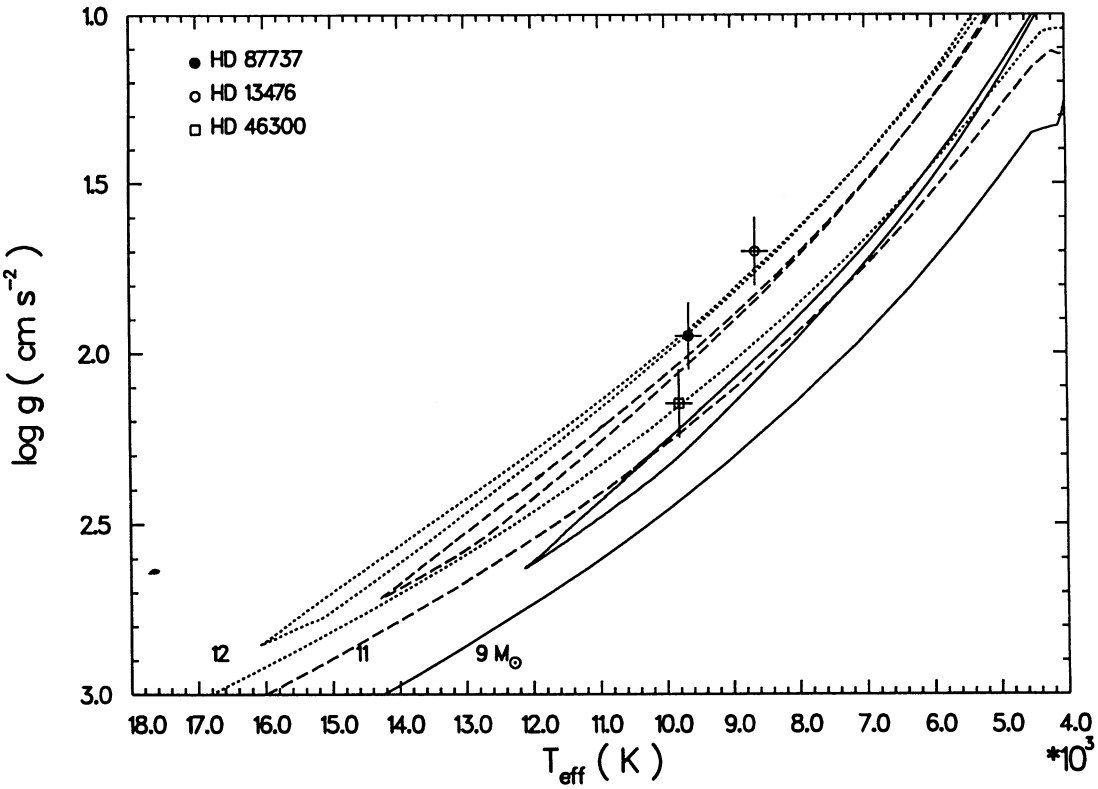

Fig. 5.—Comparison of the log g and $T_{\rm eff}$ values of the three A-type supergiants listed in Table 3A with the present evolutionary tracks of the 9, 11, ad 12 $M_\odot$ stars. The observed stars seem to have masses 10–12 $M_\odot$.

does not lead to significantly different results in this mass range.

The conclusion from this comparison is as follows: On the basis of our predicted surface abundances and the evolutionary tracks, we may consider the observed stars in Table 3A as post–red supergiants performing blue loops in the H-R diagram. However, the N enrichment inferred from the observational analysis is generally larger than predicted. It is not clear how to resolve this discrepancy, because the observational situation is not yet settled. For example, considering the star HD 87737 (η Leo), a value [N/H] = +0.27 has been derived by TT94, compared to [N/Fe] = +0.78 according to Venn (1993). (Note that both quantities are equal when [Fe/H] = 0.) As emphasized by Venn (1993), the observed high nitrogen enhancement may indicate a large systematic error in the classical analysis of the N I lines in A supergiant atmospheres (large non-LTE correction). Therefore, we argue again that more observations are needed for A-type supergiants in order to determine whether additional mixing of CNO-processed gas is required to explain their abundance anomalies. Such stars are indeed very important in order to understand the complex nuclear and mixing history in massive stars.

6. CONCLUDING REMARKS

In this work, we have investigated the contribution of the Ne-Na cycle to the production of ^{23}Na in stars of initial masses $M = 5$–$19\ M_\odot$. We have compared our predictions for the Na excess with the values recently derived for a sample of A–F type supergiants (see Table 1). On the basis of this comparison, the following conclusions can be drawn.

1. Our stellar models lead to values of the Na excess, [Na/H], which are compatible with the moderate values observed for the F-type supergiants (see Fig. 3). The positions of the majority of these stars in the log g-log $T_{\rm eff}$ diagram were found to be consistent with our evolutionary tracks (see Fig. 4). This means that they may be considered as post–red supergiants which have evolved through the first dredge-up phase and are upon the blue loops in the H-R diagram. This view seems to be supported by the correlation we have found (see Fig. 2) between [Na/H] and [Na/H], which was also suggested on observational basis.

Obviously the existence of the blue loops, as seen in Figure 1, is required for this interpretation. Referring to the brief discussion in § 4 and to the detailed description in the paper by El Eid (1994b), it has been found that these loops were suppressed for stellar masses of $M > 13\ M_\odot$ when the Schwarzschild criterion for convection was used in the model computation. However, these loops were recovered when the Ledoux criterion was adopted and combined with semiconvective mixing. This behavior has been related to the efficiency of mixing in the layers where the hydrogen-burning shell operates during core He buring.

Our successful explanation of the Na excess in several F-type supergiants requires the existence of the blue loops and implies that, in the case of stars with $M > 13\ M_\odot$, mixing in these layers may not be as efficient as obtained on the basis of the Schwarzschild criterion. Therefore, we may conclude that the interpretation of the abundance anomalies, in particular that of Na, represents a very useful tool for testing the treatment of mixing processes in massive stars of $M \geq 13\ M_\odot$.

2. It is still not clear how to explain the large values [Na/H] $\sim$ +0.80–1.0 suggested for the A-type supergiants. More observations and better statistics are certainly needed for the A-type supergiants in order to understand their evolutionary status and abundance anomalies.

Portions of this work performed during visits by M. F. E. to Clemson University were supported by the W. M. Keck Foundation. This work was also supported by the US Department of Energy. M. F. E. thanks D. D. Clayton and D. Hartmann for their support and encouragement, and has appreciated many comments and discussions with N. Prantzos. We also thank Prof. C. de Jager for many valuable remarks.

APPENDIX

REACTION RATES FOR THE NeNa CYCLE

All of the reactions in the NeNa cycle have been measured, and corresponding thermonuclear reaction rates may be found in CF88. Little in the way of new experimental information has been reported since this compilation and several of the rates remain rather uncertain at low temperatures. Consequently, we have reexamined all of these rates to determine their reliability and, in some cases, to offer improved estimates. However, significant uncertainties remain for low temperatures which is of consequence not only for this study, but also for Na abundances in the globular clusters. The rates that we list are appropriate for temperatures $T_9 \leq 2.0$.

A1. ^{20}Ne$(p, \gamma)^{21}$Na

The ^{20}Ne$(p, \gamma)^{21}$Na reaction is noteworthy because, at very low temperatures, its rate is dominated by capture through the tail of a state located 6.5 keV *below* the (p, γ) threshold. Rolfs et al. (1975) have measured cross sections for this subthreshold resonance as well as those for nonresonant direct capture (DC), and for several low-energy resonances. Other resonance strengths have been tabulated by Endt & van der Leun (1978). These data form the basis for the rate given in CF88. However, the accepted (p, γ) Q-value is now about 0.5 keV lower than it was when these rates were calculated (Endt 1990). As a result, we have adjusted the reaction rate to account for the revised Q-value:

$$\begin{aligned} N_A\langle\sigma v\rangle = {} & 2.05 \times 10^8 T_9^{-2/3} \exp(-19.452/T_9^{-/3})\{1 + 2.67 \exp[(-T_9/0.21)^{1/2}]\} \\ & + 9.55 \times 10^6 \exp(-19.452/T_9^{1/3})/[T_9^2(1 + 0.0116/T_9^{2/3})^2] \\ & + 18.0 T_9^{-3/2} \exp(-4.257/T_9) + 9.83 T_9^{-3/2} \exp(-4.619/T_9) \\ & + 1.59 \times 10^5 T_9^{-1.49} \exp(-12.908/T_9)\ \text{cm}^3\ \text{s}^{-1}\ \text{mole}^{-1}. \end{aligned} \quad \text{(A1)}$$

The first two terms describes the contributions from DC and the -6.5 keV resonance, respectively; the third and fourth terms are due to resonances at center-of-mass energies $E_{cm} = 367$ and 398 keV, respectively; while the last term accounts for higher energy resonances. This rate is accurate to $\pm 12\%$–15% for $T_9 < 0.4$, and within errors, is indistinguishable from that appearing in CF88.

A2. ^{21}Ne$(p, \gamma)^{22}$Na

Resonances in the ^{21}Ne$(p, \gamma)^{22}$Na reaction have been measured (Berg et al. 1977; Keinonen, Riihonen, & Anttila 1977; Görres et al. 1982, 1983; Becker et al. 1992) down to $E_{cm} = 121$ keV. Two states below this energy are known to exist. Of these, only the uppermost state, at $E_{cm} = 96$ keV (corresponding to an excitation energy $E_x = 6834$ keV), is located at an astrophysically interesting energy. In this energy region, the resonance strength is simply proportional to the proton width (since $\Gamma_p \ll \Gamma_\gamma$). This quantity was estimated by Görres et al. (1983) who assumed a proton spectroscopic factor $C^2S \leq 1$. However, since this state is only weakly populated in the ^{21}Ne(^{3}He, d)^{22}Na reaction (Garrett, Middleton, & Fortune 1971a), an upper limit of $C^2S = 1$ is unrealistically large. The 6834 keV state is thought to be analogous to a state in ^{22}Ne at 6240 keV (Garrett et al. 1971b). From measurement of the ^{21}Ne$(d, p)^{22}$Ne reaction with reasonable energy resolution (Heikkinen et al. 1972; Neogy, Middleton, & Scholz 1972), we estimate a conservative upper limit of $C^2S \leq 0.05$ for the analog pair. We obtain the proton width from the usual relation $\Gamma_p = C^2S\,\Gamma_{sp}$ where Γ_{sp} is the single-particle width which we calculate using a realistic, diffuse nuclear potential. The resulting upper limit on the resonance strength is $\omega\gamma = 2.2 \times 10^9$ eV.

From the available experimental results, we recommend the following reaction rate:

$$N_A\langle\sigma v\rangle = 3.4 \times 10^8 T_9^{-2/3} \exp(-19.41/T_9^{1/3})\{1 + 0.56 \exp[-(16.7T_9 - 1)^2]\} + 6.12T_9^{-3/2} \exp(-1.403/T_9) + 1.35 \times 10^4 T_9^{-3/2} \exp(-3.008/T_9) + 3.12 \times 10^6 T_9^{-0.72} \exp(-8.268/T_9^{0.67}) + [0\text{–}1]1.1 \times 10^{-3} T_9^{-3/2} \exp(-1.114/T_9)\ \mathrm{cm^3\ s^{-1}\ mole^{-1}}\ . \quad \text{(A2)}$$

The first three terms are from Görres et al. (1982) and represent the nonresonant, and $E_{cm} = 121$ and 259 keV resonances, respectively. The fourth term accounts for higher energy resonances and was calculated from a weighted average of the published resonance strengths. The final term describes the possible contribution of the 96 keV resonance. The *upper* limit of this rate is almost identical to the *lower* limit appearing in CF88 because the 96 keV resonance now has an almost negligible effect on the total rate. Its maximum contribution occurs near $T_9 = 0.03$ where it increases the rate by at most 40%.

A3. ^{22}Ne$(p, \gamma)^{23}$Na

In contrast with the two reactions discussed above, the ^{22}Ne$(p, \gamma)^{23}$Na reaction is poorly determined at low temperatures. Numerous resonances have been measured, and these results have been tabulated by Endt (1990). However, as many as 14 states are thought to lie below the lowest measured resonance (at $E_{cm} = 418$ keV). Two of these states have been observed in proton-stripping studies (Powers, Fortune, & Middleton 1971; Childs et al. 1973) and they therefore correspond to (p, γ) resonances at 36 and 151 keV. One state is reported to lie 8 keV below the 36 keV resonance, but it appears to be an artifact of different measurements of the latter state. We again use a diffuse nuclear potential to describe the single-particle states and take an average of the published spectroscopic factors to calculate Γ_p for these two states. Our widths are somewhat smaller than those reported by Görres et al. (1983), but we believe our calculation to be more realistic.

This leaves 11 states that have not been observed in either (p, γ) (Görres et al. 1982) or proton stripping (Powers et al. 1971; Childs et al. 1973). Upper limits on resonance strengths and proton spectroscopic factors were obtained by Görres et al. (1982, 1983). These limits are sufficient to eliminate nine of the 11 states from further consideration. The remaining two states could correspond to resonances located at 68 and 100 keV. We have calculated upper limits for their resonance strengths using the procedure outlined above. The resulting ^{22}Ne$(p, \gamma)^{23}$Na reaction rate is

$$N_A\langle\sigma v\rangle = 1.05 \times 10^9 T_9^{-2/3} \exp(-19.431/T_9^{1/3}) + 1.24 \times 10^{-9} T_9^{-3/2} \exp(-0.414/T_9) + 0.029T_9^{-3/2} \exp(-1.752/T_9) + 9.30 \times 10^4 T_9^{-1.174} \exp(-5.100/T_9) + 5.71 \times 10^5 T_9^{-0.249} \exp(-7.117/T_9) + [0\text{–}1]3.25 \times 10^4 T_9^{-3/2} \exp(-0.789/T_9) + [0\text{–}1]0.10T_9^{-3/2} \exp(-1.161/T_9)\ \mathrm{cm^3\ s^{-1}\ mole^{-1}}\ . \quad \text{(A3)}$$

The first three terms represent DC (Görres et al. 1983), and the 36 and 151 keV resonances, respectively. The next two terms together are the contribution of resonances for $E_{cm} \geq 417$ keV. The final two terms describe the possible resonances at 68 and 100 keV.

The *lower* limit for this rate is some 5–30 times the *upper* limit suggested by CF88 for $T_9 = 0.2$–0.5. This is because the lowest resonance was originally placed at 30 keV rather than at 36 keV. This small energy difference translates into a large difference in resonance strengths. Unfortunately, the [0–1] terms listed above produce sizeable uncertainties which grow from a factor of 2 at $T_9 = 0.03$ to a factor of 3400 by $T_9 = 0.08$. High resolution proton-stripping measurements will be required to reduce these uncertainties. However, the evidence that either of these states actually exist is tentative at best. Therefore it is likely that the actual rate will turn out to be near its present lower limit.

A4. ^{23}Na$(p, \alpha)^{20}$Ne AND ^{23}Na$(p, \gamma)^{24}$Mg

There are several states known to exist between the ^{23}Na + p threshold and the lowest observed resonance at $E_{cm} = 171$ keV (Zyskind, Rios, & Rolfs 1981; Görres, Wiescher, & Rolfs 1989; Endt 1990). These states could correspond to resonances at 4, 36, and 137 keV. The 4 keV resonance is too low in energy to have any significant impact on the reaction rate, but the other two states may contribute if they have sufficiently large proton widths. Estimates of resonance strengths have been made (Zyskind et al. 1981; Görres et al. 1989) by assuming that these states are pure single-proton states. However, the state corresponding to the 36 keV

resonance ($E_x = 11.727$ MeV) has $J^\pi = 0^+$, and Garrett et al. (1978) have shown that the known 0^+ bandheads are very weakly populated in proton-transfer reactions. From the (d, n) spectrum published by Fuchs et al. (1968), we estimate a proton spectroscopic factor $C^2S \leq 0.6$ for this state. Similarly, by assuming s-wave transfer we estimate $C^2S \leq 0.1$ for the 137 keV resonance ($E_x = 11.828$ MeV).

The tabulated (Endt 1990) width and (α, γ) resonance strength for the 11.727 MeV state imply $\Gamma_\gamma = 0.37$ eV and $\Gamma_\alpha = 10$ keV. Our limit on the proton spectroscopic factor is consistent with $\Gamma_p \leq 4.9 \times 10^{-18}$ eV. Hence $\omega\gamma_{(p,\alpha)} \leq 6.1 \times 10^{-19}$ eV and $\omega\gamma_{(p,\gamma)} \leq 2.3 \times 10^{-23}$ eV for the 36 keV resonance. Similar width information does not exist for the 11.828 MeV state. Therefore, we assume $\Gamma_\alpha/\Gamma = 1$ in order to provide an upper limit for the (p, α) reaction and $\Gamma_\gamma/\Gamma = 1$ for the (p, γ) case. These choices, combined with $\Gamma_p \leq 2.3 \times 10^{-9}$ eV and a maximum spin $J = 2$, yield $\omega\gamma \leq 1.4 \times 10^{-9}$ eV for both reactions. We have also recalculated the contribution to the cross section from the tails of higher energy resonances and find the following thermonuclear reaction rate for the (p, α) reaction:

$$N_A\langle\sigma v\rangle = 1.26 \times 10^{10} T_9^{-2/3} \exp\left[(-20.758/T_9^{1/3}) - (T_9/0.13)^2\right](1 + 0.02T_9^{1/3} - 13.8T_9^{2/3} - 1.93T_9 + 234T_9^{4/3} + 83.6T_9^{5/3}) + 4.38T_9^{-3/2} \exp(-1.979/T_9) + 6.50 \times 10^6 T_9^{-1.336} \exp(-6.490/T_9) + 1.19 \times 10^8 T_9^{-1.055} \exp(-11.411/T_9) + [0\text{–}1]9.91 \times 10^{-14} T_9^{-3/2} \exp(-0.418/T_9) \text{ cm}^3 \text{ s}^{-1} \text{ mole}^{-1} . \quad \text{(A4)}$$

The first term describes the tails of high-energy resonances and is 40%–100% larger than the comparable expression in CF88. The next term represents the 171 keV resonance (Zyskind et al. 1981; Görres et al. 1989), and the following two terms describe the integrated contribution of higher energy resonances (Endt 1990). Finally, the [0–1] term is the upper limit on the contribution of the 36 keV resonance. The 137 keV resonance has little influence on the rate. Our lower limit is within a factor of 2 of that appearing in CF88 for $T_9 \leq 0.2$. However, our upper limit is only 10%–27% of the upper limit in CF88 for $T_9 \leq 0.04$.

For the (p, γ) reaction, we have used the estimated strengths described above along with the tabulated strengths for higher energy resonances found in Endt (1990). We have also estimated the DC contribution using the model of Rolfs (1973) and tabulated spectroscopic factors for the bound states of ^{24}Mg (Endt 1990). This calculation yields an approximately constant S-factor of 0.47 MeV b. However, this result is uncertain by at least 50% owing to the rather large uncertainties found in the spectroscopic factors. The resulting (p, γ) reaction rate is

$$N_A\langle\sigma v\rangle = 2.47 \times 10^9 T_9^{-2/3} \exp(-20.758/T_9^{1/3}) + 91.9T_9^{-3/2} \exp(-2.789/T_9) + 1.72 \times 10^4 T_9^{-3/2} \exp(-3.433/T_9) + 3.44 \times 10^4 T_9^{0.323} \exp(-5.219/T_9) + [0\text{–}1]2.34 \times 10^{-4} T_9^{-3/2} \exp(-1.590/T_9) \text{ cm}^3 \text{ s}^{-1} \text{ mole}^{-1} . \quad \text{(A5)}$$

The first three terms account for DC and resonances at 240 and 296 keV, respectively. The next term describes higher energy resonances while the last term is the upper limit for the 137 keV resonance. Unlike the (p, α) case, neither the 36 keV resonance nor resonance tails have a significant effect on the (p, γ) reaction rate. The present rate is uncertain by about a factor of 2 near $T_9 = 0.08$. Otherwise, the upper and lower limits are essentially identical. At low temperatures ($T_9 \leq 0.06$), this rate is 3–4.7 times what is found in CF88.

REFERENCES

Anders, E., & Grevesse, N. 1989, Geochem. Cosmochem. Acta, 53, 197
Becker, H. W., et al. 1992, Z. Phys., A343, 361
Berg, H. L., Hietze, W., Rolfs, C., & Winkler, H. 1977, Nucl. Phys., A276, 168
Boyarshuck, A. A., Gubney, I., Kubat, I., Lyubimkov, L. S., & Sakhibullin, N. A. 1988, Astrofizika, 28, 335 (1989, Astrophysics, 29, 197)
Bressan, F., Fagotto, G., Bertelli, G., & Chiosi, C. 1993, A&AS, 100, 647
Caughlan, G. R., & Fowler, W. A. 1988, Atomic Data Nucl. Data Tables, 40, 284 (CF88)
Caughlan, G. R., Fowler, W. A., Harris, M. J., & Zimmerman, B. A. 1985, Atomic Data Nucl. Data Tables, 32, 197
Childs, W. A., Ritter, R. C., Murphy, B. D., & Strang, R. M. 1973, Nucl. Phys., A203, 133
de Jager, C., Nieuwenhuijzen, H., & van der Hucht, K. 1988, A&AS, 72, 259
Denissenkov, P. A. 1990, Astrophysics, 31, 588
El Eid, M. F. 1994a, A&A, 285, 915
———. 1994b, MNRAS, in press
El Eid, M. F., & Prantzos, N. 1993, in Origin and Evolution of the Elements, ed. N. Prantzos, E. Vangioni-Flam, & M. Cassé (Cambridge: Cambridge Univ. Press), 279
Endt, P. M. 1990, Nucl. Phys., A521, 1
Endt, P. M., & van der Leun, C. 1978, Nucl. Phys., A310, 1
Fuchs, H., Grabish, K., Kraatz, P., & Röschert, G. 1968, Nucl. Phys., A122, 59
Garrett, J. D., Fortune, H. T., Middleton, R., & Scholz, W. 1978, Phys. Rev., C5, 2032
Garrett, J. D., Middleton, R., & Fortune, H. T. 1971a, Phys. Rev., C4, 165
Garrett, J. D., Middleton, R., Pullen, D. J., Anderson, S. A., Nathan, O., & Hansen, O. 1971b, Nucl. Phys., A164, 449
Görres, J., et al. 1983, Nucl. Phys., A408, 372
Görres, J., Rolfs, C., Schmalbrock, P., Trautvetter, H. P., & Kienonen, J. 1982, Nucl. Phys., A385, 57
Görres, J., Wiescher, M., & Rolfs, C. 1989, ApJ, 343, 365
Heikkinen, D. W., Lutz, H. F., & Bartolini, W. 1972, Nucl. Phys., A193, 372
Iglesias, C. A., Rogers, F. J., & Wilson B. G. 1992, ApJ, 397, 717
Keinonen, J., Riihonen, M., & Anttila, A. 1977, Phys. Rev., C15, 579
Kippenhahn, R., & Weigert, A. 1990, Stellar Structure and Evolution (Berlin: Springer)
Landré, V., Prantzos, N., Auger, P., Bogaert, G., Levebre, A., & Thibaud, K. P. 1990, A&A, 240, 85
Lobel, A., de Jager, C., Nieuwenhuijzen, H., Smolinski, J., & Gesicki, K. 1994, A&A, 291, 226
Luck, R. E., & Lambert, D. L. 1985, ApJ, 298, 782
Mowlavi, N., & Foristini, M. 1994, A&A, 282, 843
Neogy, P., Middleton, R., & Scholz, W. 1972, Phys. Rev., C6, 885
Powers, J. R., Fortune, H. T., & Middleton, R. 1971, Phys. Rev. C4, 2030
Prantzos, N., Coc, A., & Thibaud, J. P. 1991, ApJ, 379, 729
Robertson, J. W. 1972, ApJ, 177, 473
Rolfs, C. 1973, Nucl. Phys. A217, 29
Rolfs, C., Rodney, W. S., Shapiro, M. H., & Winkler, H. 1975, Nucl. Phys., A241, 460
Schaller, G., Schaerer, D., Meynet, G., & Maeder, A. 1992, A&AS, 96, 269
Stothers, R. B., Chin, C.-W. 1994, ApJ, 431, 797
Takeda, Y., & Takada-Hidai, M. 1994, PASJ, 46, 395 (TT94)
Venn, K. A. 1993, ApJ, 414, 316
Weaver, T. A., & Woosley, S. E. 1993, Phys. Rep., 227, 65
Woosley, S. E., & Weaver, T. A. 1988, Phys. Rep., 163, 79
Zyskind, J., Rios, M., & Rolfs, C. 1981, ApJ, 243, L53; 245, L97